Fundamentals of Liquid Phase Sintering During Selective Laser Sintering

D. E. Bunnell*, S. Das*, D. L. Bourell*, J. B. Beaman*, and H. L. Marcus†

*Center for Material Science & Engineering, University of Texas at Austin, Austin TX 78712
†Institute for Materials Science, University of Connecticut, Storrs CT 06269-3136

Introduction

One of the advantages of the Selective Laser Sintering (SLS) process is that a variety of materials can be processed. However, the goal of being able to produce fully dense metal parts with no post processing has been elusive. Using Selective Laser Sintering to produce metal parts with full density without post processing poses a challenge since both the processing conditions and the metal system must be controlled. This article describes two metallurgical mechanisms by which loose metal powder beds could be sintered to nearly full density using a scanning laser beam. The mechanisms are particle rearrangement during liquid phase sintering (LPS) and in-situ infiltration. Some of the particles, when heated by the laser radiation, melt and form a liquid. If this liquid has certain physical properties (e.g., low viscosity and high surface tension) and wets the other solid particles, then the SLS process can in theory produce dense layers by either mechanism. The purpose of this study is to determine the process and material selection parameters required to achieve fully dense parts during direct Selective Laser Sintering of metal.

Test Methods

Several low melting point metals were tested to determine if they could produce full density SLS parts. Two nickel brazes, BNi-6 and BNi-7, were selected because of their relatively high melting temperatures of 875°C and 890°C. In addition, three tin based solders, 63Sn-37Pb, 50Sn-50Pb, and 96Sn-4Ag were selected because of their low melting temperatures. The nickel brazes were obtained from the Wall Colmonoy Corporation and carry their designation of Nicrobraz 10 for the BNi-6 and Nicrobraz 50 for the BNi-7. The composition of Nicrobraz 10 is 11P-89Ni and the composition of Nicrobraz 50 is 14Cr-10P-Ni balance.

The rate of liquid infiltration into three dimensional porous media is known to depend on the liquid-vapor surface tension γ_{lv}, liquid viscosity η, and particle size d [1]. We measured γ_{lv} using one of two methods, the pendant drop for high melting temperature alloys and the sessile drop for low melting point alloys.

The pendant drop weight method for determining surface tension was used for the high melting temperature alloys because no contamination from a substrate is added to the material being tested as the drop is formed homogeneously at the end of the rod. The liquid-vapor surface tension γ_{lv} can be determined by measuring the weight of a pendant drop after it has separated from the rod . As a drop forms at the end of a rod, the weight of the liquid drop is balanced by the surface tension. When the drop separates from the rod, some fraction of the liquid remains on the rod. The surface tension can be calculated as:

$$\gamma_{lv} = m_o \, g \, F/R_1 \qquad (1)$$

where m_o is the mass of an "ideal" drop that completely separated from the rod, g is the gravitational constant, F is the correction to account for the fraction of the "ideal" drop that actually separates, and R_1 is the radius of the solid rod. The factor F is related to $R_1/V^{1/3}$ (where V is the volume of the drop after it has separated from the rod) and is empirically fitted to the equation:

$$F = 0.14782 + 0.27896\,(R_l/V^{1/3}) - 0.166(R_l/V^{1/3})^2 \quad (2)$$

where V is the volume of a drop and is calculated from the weight of a drop divided by the liquid density.

To use the pendant drop method, the material being tested must be in rod form. Since Wall-Colmonoy Nicrobraz 10 and 50 are only available in powder form, rods of the material were vacuum cast. The powder was placed in a 3.0 mm I.D. glass tube with one end sealed, the tube was evacuated using a mechanical pump, and the other end of the tube was sealed using a propane torch. The tubes were placed in a furnace operating at 900°C and the powder melted and fused together into a rod. The glass simultaneously softened and, due to the pressure differential, collapsed around the liquid. After cooling, the glass sheath was removed from the metal rod.

Figure 1 is a sketch of the apparatus used to measure the surface tension of different materials using the pendant drop technique. A rod of the material being tested was suspended from the bottom hook of the balance and the furnace was raised using a lab jack to heat the end the rod. As drops fell from the rod the weight indicated on the balance decreased by the weight of each drop. A computer program was written to interface with the balance and detect the weight change, average the drop weight, and calculate the surface tension.

The low melting temperature alloys could be tested using a hot plate in a vacuum chamber. Glass microscope slides were used as the substrates for the sessile drop measurements. A 35 mm SLR camera with a 150 mm focal length lens and a 7x "close-up kit" lens assembly was used to photograph the drops. The chamber was evacuated and back-filled with premixed 4% H_2 in nitrogen.

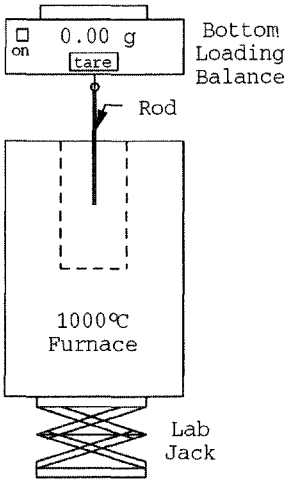

Figure 1. Pendant drop-weight apparatus for determining surface tension

Figure 2 is a sketch of a sessile drop defining the values of the drop diameter d_m, the height of the drop from the maximum diameter to the top of the drop H, and the distance H', from the top of the drop to the intersection of the axis with a 45° tangent to the drop. There are two equations that can be used to measure the surface tension from the dimensions of a sessile drop, but only one is applicable to small drops where the top surface is not flat. The Dorsey equation was used to calculate the surface tension from the curvature of a sessile drop [2]. The Dorsey equation is:

$$\gamma_{lv} = \frac{g\,\rho\,d_m^2}{4}\left(\frac{0.0520}{f} - 0.1227 + 0.0481\,f\right) \quad (3)$$

where the Dorsey factor f is given by

$$f = \frac{2H'}{d_m} - 0.4142 \quad (4)$$

The viscosity of the liquid solders was measured using a capillary flow tube. Figure 3 is a schematic drawing of the viscometer. The viscometer was constructed from an insulated graphite rod machined to form a reservoir above an alumina capillary tube. A quartz powder suspension in butanol was applied the exposed surfaces of the graphite to keep the graphite from oxidizing in the furnace. The quartz layer was not wet by the liquid metal and also prevented the liquid metal from reacting with the graphite. The viscometer was placed in a furnace and allowed to soak for one

hour prior to testing. The viscometer was then removed from the furnace and supported over a small collection vial of known volume. A tapered 2 mm graphite rod was used to plug the capillary tube while liquid metal was poured into the reservoir. The tapered rod was removed to allow molten metal to flow through the capillary. The time to fill the vial was recorded.

The viscometer was calibrated using the known viscosity of liquid mercury and molten gallium metal. The equation used to calibrate the viscometer was:

$$\eta = \frac{\pi t r^4 P}{8 V L} + \frac{n V \rho}{8\pi t L} \qquad (5)$$

where η is the viscosity of the liquid, r is the inner diameter of the capillary tube, P is the pressure head, t is the time, V is the volume of liquid passing through the tube in time t, L is the length of the tube, n is a calibration constant, and ρ is the density of the liquid.

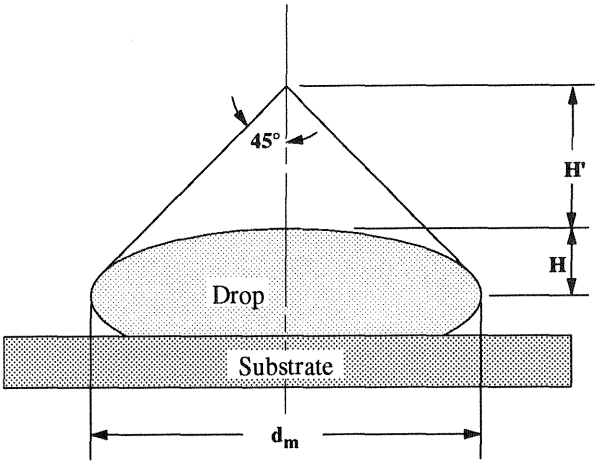

Figure 2. Sketch of a sessile drop showing relationship of height and diameter used for the Dorsey equation (Equation 3) to calculate surface tension

The infiltration rate of a liquid into a thin powder bed was measured by depositing a liquid onto the top surface of a thin powder layer. Water and n-butyl alcohol where deposited on 1.0 and 0.3 mm thick layers of 100 mesh and 325 mesh metal powders. After a relationship between spreading rate and surface tension, viscosity, powder size, drop volume, and layer thickness was determined, the spreading rate of molten solder in copper powder was measured to validate the relation for metals.

To tie the infiltration relationship to the SLS process, a series of tests were conducted in which a CO_2 laser beam was focused at different locations on a powder bed of 80% BNi-6 and 20% 1018 steel for short periods of time. Scanning mirrors directed the laser beam to a location, dwell on the spot for a short time and then jump to the next programmed location where the process was repeated with increasing dwell times. Three laser powers were tested: 10, 20, and 30 watts. The dwell time at each location was increased from zero seconds to 1.5 seconds by 0.25 second increments. After a series of sintered spots were created, a quick setting epoxy was applied to the bed and allowed to cure so the spots could be microsectioned. The infiltrated metal beneath the spots was examined using optical microscopy to determine the density and infiltration characteristics of the liquid into the metal powder bed under the laser spot.

Results

The pendant drop experiments on BNi-6 indicated that the surface tension of this alloy in an atmosphere of premixed 96% N_2 - 4% H_2 with a residual of 1.7% oxygen from air, is 1360 mN/m at its melting temperature of 875° C. The value of the surface tension of BNi-6 in 96% N_2 - 4% H_2 with 2.0% oxygen from air decreases to 1300 mN/m. When the residual oxygen was reduced to 0.7% by purging the glovebox with more premixed 96% N_2 - 4% H_2 the surface tension of the BNi-6 increased to 1580 mN/m. When the oxygen content was reduced further to 0.3% the surface tension increased again to a value of 1600 mN/m.

Surface tension measurements using the pendant drop method were not possible on BNi-7 alloy because the outer surface of the rod formed a oxide film that prevented the formation of droplets at

the temperature (1000°C) and oxygen partial pressures (less than 0.1% oxygen in 96% N_2 - 4% H_2) present in the glovebox furnace.

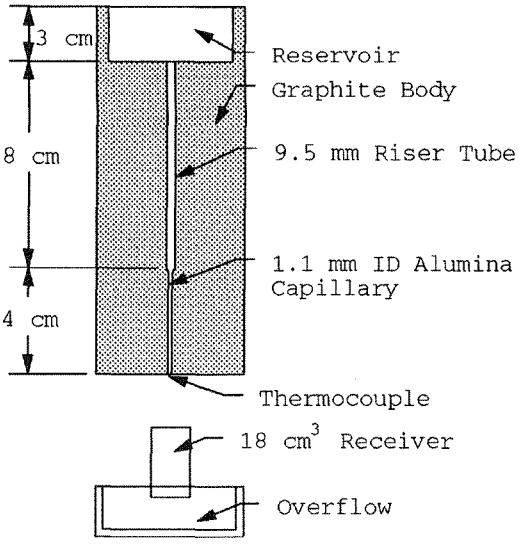

Figure 3. Viscometer used to determine viscosity of liquid metals

The surface tension of a liquid can be calculated at any temperature above the melting point (but below the boiling point) using the sessile drop test. However, this requires measuring the density of the liquid at the temperature of the surface tension test. Figure 4 is a graph of the data collected on the densities of three solders at various temperatures. Sessile drop experiments indicated surface tensions of 50Sn-50Pb, 63Sn-37Pb, and 96Sn-4Ag solders to be 360, 370, and 440 mN/m, respectively. The literature value for the surface energy of 63Sn-37Pb in a vacuum is 492 mN/m [3]. The surface tension values reported here are lower than reported in the literature. This difference is perhaps due to the oxygen contamination in the chamber of about 0.1%. Although an attempt was made to calculate the change in surface tension with changing temperature $d\gamma/dT$, there was no statistically significant change of γ_{lv} in the temperature range of 200° to 350°C. The literature value for the $d\gamma/dT$ of 63Sn-37Pb in a vacuum is 0.09 mN/m $°C^{-1}$ which is too small for us to detect in the data scatter. The surface tension data are presented graphically in Figure 5. The lack of a definite decrease in surface tension with increasing temperature is apparent.

A model for the infiltration rate of a liquid into a thin powder layer was empirically developed from liquid spreading into a thin layer of metal powder. The test parameters were: the layer thickness, the amount of liquid initially present, the particle size, the viscosity of the liquid, and the surface tension of the liquid. After data analysis, it was determined that the layer thickness and initial amount of liquid deposited on the top of the layer had no statistically significant impact on the radial rate of liquid infiltration. The distance r the infiltration front advances in a radial direction is given by:

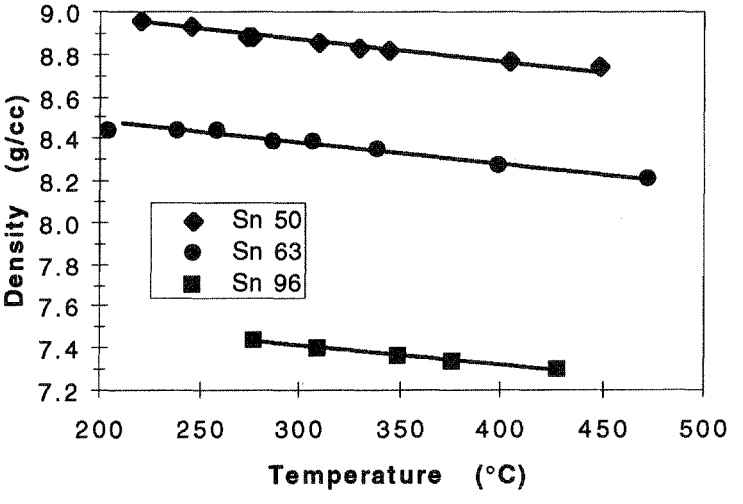

Figure 4. Density variations of solder with temperature

$$\text{radius} = 6.0 \cdot 10^{-5} \ (\text{time})^{0.5} \left(\frac{\gamma_{lv}}{\eta}\right)^{2.0} (\text{diameter})^{-0.5} \qquad (6)$$

where the radius of the advancing front is given in centimeters, time is in seconds, γ_{lv} has units of mN/m, η has units of mPa·s, and the particle diameter has units of micrometers.

Data from the solder spreading in copper powder are graphed in Figure 6. The solid lines represent equation 6 with the corresponding viscosity, surface tension, and particle size values. The data for Sn63 did not fit the equation due to the uneven radial spreading of the solder into the copper bed for that experiment.

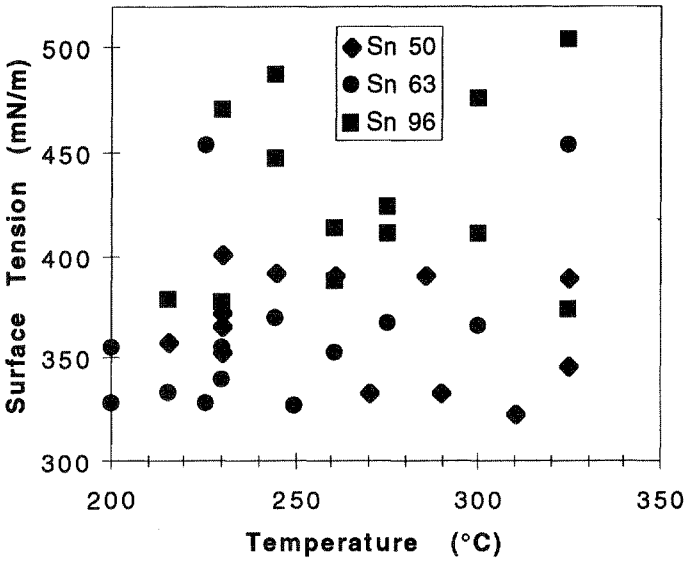

Figure 5. Surface tension data from sessile drop tests for solder

Discussion

Selective Laser Sintering of metal parts poses a challenge because both the processing conditions and the metal system must be controlled. The laser beam must be controlled so that only the low melting point particles melt. If there is too much liquid, created either by melting the high melting temperature particles or by the formation of a liquid solution, the powder in the layer will tend to form spherical balls. It is critical that the liquid phase wet the solid phase completely and rapidly during the SLS process. Since a liquid phase must be generated that wets the solid phase, both the solid and liquid phases must be selected so that their surface energies assure wetting and rapid capillary flow. The solubility of the solid phase into the liquid should be as low as possible consistent with rapid, complete wetting. The liquid phase must have a low viscosity so that the liquid can infiltrate the solid particles rapidly. The liquid phase should have a lower absorbance to the laser radiation than the solid so that the solid particles will be hotter than the liquid. This will promote capillary flow and rapid wetting while reducing the tendency of the liquid to form spheres.

Whether a liquid will wet a solid is determined by equilibrium thermodynamics. Young's equation [4,5] for wetting was developed from a mechanistic approach of balancing horizontal components of the three interfacial energies at equilibrium:

$$\gamma_{sv} - \gamma_{ls} = \gamma_{lv} \cos\theta \qquad (7)$$

where γ_{sv} is the solid-vapor interfacial energy, γ_{ls} is the liquid-solid interfacial energy, γ_{lv} is the liquid-vapor interfacial energy, and θ is the contact angle the liquid makes with the solid. In both the pendant drop and sessile drop tests, the system was assumed to be at mechanical and chemical equilibrium; i.e., the interface was static and there were no chemical reactions. Since the system was at or near equilibrium, neither the value of the contact angle nor the surface energy of the liquid changed with time.

A liquid metal will tend to form droplets unless there is a solid that the liquid can wet and infiltrate into or spread over. The infiltration model presented in equation 6 implies that the ratio of surface tension to viscosity γ_{lv}/η should be as high as possible for the liquid to rapidly infiltrate the powder bed. The viscosity of liquid metals varies from about 0.2 mPa·s for alkali metals to around

5 mPa·s for d-transition metals [6-8]. The surface tension of liquid metals encompasses the range of 1800 mN/m for d-transition metals to around 300 mN/m for the alkali metals and semi-metals [9]. A good low melting temperature metal for SLS processing would have high surface tension, but not higher than the high melting temperature metal, and a low viscosity. Since oxides reduce the surface tension and increase the viscosity of liquid metals, their formation must be avoided.

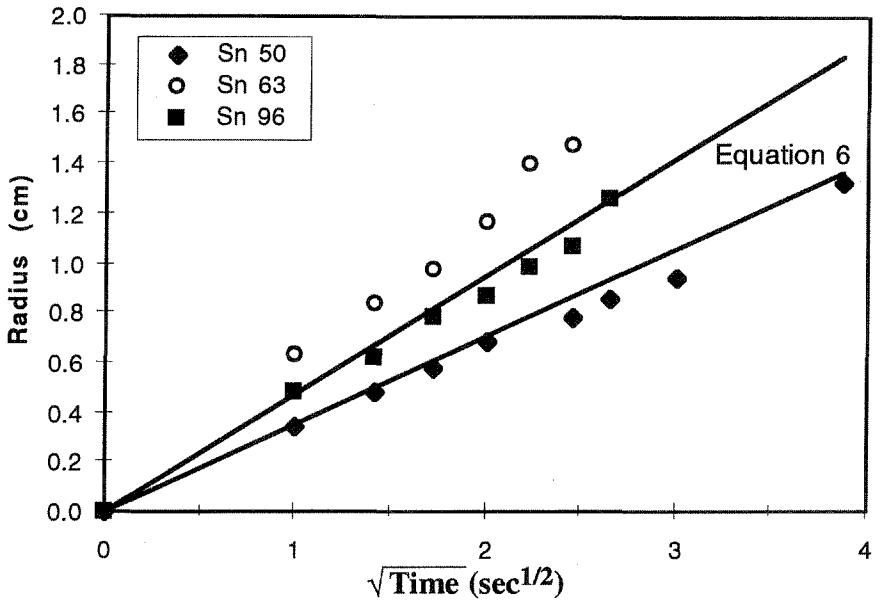

Figure 6. Solder spreading in copper powder

Another condition for the metal SLS process to be successful is that the ratio of liquid to solid must be controlled so that there is sufficient liquid to form a continuous infiltration front to sweep porosity from the powder bed. Additionally, sufficient solid particles must be present to form a solid network that the liquid can wet. If the solid particles do not form a relatively rigid network, the liquid will form spheres with solid particles in suspension rather than infiltrating into the solid network. On the other hand, if there is insufficient liquid to completely displace the vapor, residual porosity will remain after the liquid solidifies. More liquid is required to displace the vapor than that calculated from simply replacing the volume fraction of vapor because the liquid must completely encapsulate the solid and form a high solids content suspension. The amount of low melting point metal required is typically in excess of 65 volume percent [10,11], almost twice the amount of liquid required to merely replace the vapor fraction.

The binary phase diagrams for nickel-phosphorous, iron-phosphorous, and nickel-iron show that there is a eutectic in both the iron-phosphorous and nickel-phosphorous system and that nickel and iron are completely miscible in each other. Because there is extensive solubility of the solid steel in the liquid braze, complete wetting is possible. The advantage of using the nickel braze rather than tin-lead solders or copper-based brazes is that there appears to be less oxide film on the nickel-phosphorous particles (judging from the lack of dross on the SLS layers), so wetting occurs very rapidly and completely. The same behavior can be achieved with solder if the mixed solder and copper powder are fluxed with a very aggressive flux (Alpha 90 or Kester SP-30).

Figure 7 shows the top surface of a 80% BNi-6 - 20% 1018 steel powder mixture that has been fused with a 30 watt CO2 laser beam. The surface is concave due to slumping of the powder layer when the liquid infiltrated the powder bed. The BNi-6 has completed displaced the vapor phase and it appears to be fully dense. The extent of infiltration by the liquid is marked by loose powder

around the perimeter of the part.

The binary phase diagrams for copper-tin, copper-lead, and tin-lead indicate that there are no common eutectics between the three systems, unlike the iron-nickel-phosphorous system; instead, there are several intermetallic compounds. The formation of intermetallic compounds may increase the viscosity of the molten solder and prevent it from infiltrating the pores of the powder bed [12].

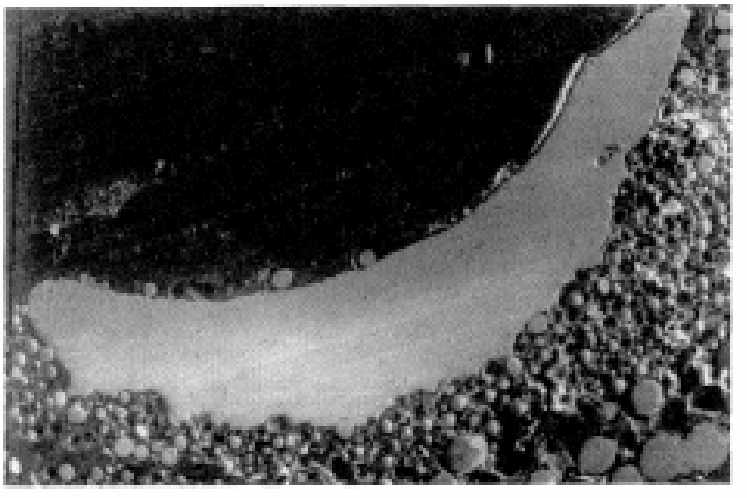

Figure 7. SEM micrograph of a 80% BNi-6 - 20% 1018 steel powder mixture that has been fused with a laser beam

The literature value for the viscosity of pure nickel is 5.2 mPa·s [6,7,13], and the Ni-P eutectic probably has a viscosity much lower than the pure element. Copper has a viscosity of 3.36 mPa·s and a surface tension of 1285 mN/m [6,7,13]. Therefore, the γ_{lv}/η parameter for copper is 382 and it should infiltrate steel powder in a similar fashion as the BNi-6 braze alloy. However, the reflectivity of atomized copper powder (as opposed to electrolytic powder) at a CO_2 laser wavelength of 10.6 μm is much higher than the reflectivity of nickel or iron [14]. For the same laser energy density, much less copper is melted, so there is less liquid formed to infiltrate the pores between the iron particles.

Conclusions

During direct metal SLS, the metal powder layer consists of low melting point particles, high melting point particles and vapor. The rate limiting factor for how fast a laser beam can scan across the metal powder bed and leave behind a fully dense area is related to the sum of the time required to melt the low melting point particles to create a liquid and the infiltration rate of the liquid metal into the powder. The vapor fraction of a powder bed must be expelled by an advancing liquid front if the gas is to be removed since diffusion of the gas through the liquid or bubbles rising through the liquid (Stoke's Law) require a longer time frame than available during Selective Laser Sintering (SLS). However, if sufficient liquid phase is present so that the front is continuous, the vapor can be displaced by the advancing liquid and the area of the metal powder bed scanned by the laser will be fully dense.

The infiltration radius r, of a liquid metal into a porous metal powder layer is given by the equation:

$$\text{radius} = 6.0 \cdot 10^{-5} \ (\text{time})^{0.5} \left(\frac{\gamma_{lv}}{\eta}\right)^{2.0} (\text{diameter})^{-0.5}$$

where the radius of the advancing front is given in centimeters, time is in seconds, γ_{lv} has units of mN/m, η has units of mN/m, and the particle diameter has units of micrometers. From this equation we can draw several conclusions regarding selecting a metal powder for the SLS process. The surface tension γ_{lv} should be as high a possible consistent with Young's equation regarding wetting of the solid. The viscosity of the liquid should be as low as possible and the particle size of the solid metal should be as small as possible.

If metal powders are selected with the appropriate surface tension, viscosity, wetting contact angle, and oxidation resistance and mixed in the appropriate ratios, it is possible to achieve fully dense SLS parts.

Acknowledgements

This study was made possible by support from a State of Texas Advanced Research Project, ATP-116: Selective Laser Sintering: Direct Metal Fabrication and ONR grant #N00014-92-J-1314.

References

1. Semlak, K.A., & Rhines, R.N.: "The rate of infiltration of metals" Trans Met Soc AIME 212 (6) 325-331 (1958)
2. Iida, T. & Guthrie, R.I.L.: The physical properties of liquid metals Clarendon Oxford (1988)
3. Murr, L.E.: Interfacial Phenomena in metals and alloys Addison-Wesley (1975) p101-107
4. Aksay, I.A., Hoge, C.E., & Pask, J.A.: "Wetting under chemical equilibrium and non-equilibrium" J. Phys. Chem 78 (12) 1178-82 (1974)
5. Hasouna, A.T., Nogi, K., & Ogino, K.: "Effects of Temperature and Atmosphere on the Wettability of Solid Copper by Liquid Tin" Trans Jap. Inst. Met. 29 (9) 748-755 (1988)
6. Beyer, R.T. & Ring, E.M.: "The viscosity of liquid metals" Liquid Metals: Chemistry and Physics Beer, S.Z. (Ed) 1972
7. Metals Handbook, Desk Edition ASM p 2.19 (1985)
8. Handbook of Chemistry and Physics 72nd Ed. CRC Press p6.169 (1991)
9. Handbook of Chemistry and Physics 72nd Ed. CRC Press p4.136 (1991)
10. German, R.M.: "Super Solidus liquid phase sintering, Part 1: Process review" Int. J. Powder Met 26 (1) 23-34 (1990)
11. Nelson, R.J. & Milner, D.R.: "Densification processes in the tungsten carbide-cobalt system" Powder Met, v15(30) 1972 p346-363
12. Manko, H.H. Solders and Soldering 3rd Ed. pp. 98-101 1992 McGraw-Hill
13. TAPP (Thermochemical And Physical Properties) version 2 for Windows. ES Microware (1994)
14. Touloukian, Y.S., & DeWitt, D.P.: Thermophysical Properties of Matter, Vol 7: Thermal Radiative Properties IFI/ Plenum Press 1970